Journal of Mathematical Research with Applications
Jul., 2024, Vol. 44, No. 4, pp. 551–568
DOI:10.3770/j.issn:2095-2651.2024.04.014
Http://jmre.dlut.edu.cn

Construction of Bézier-like Curves with Energy Constraints

Yongxia HAO*, **Hongyang LUO**
School of Mathematical Sciences, Jiangsu University, Jiangsu 212000*, P. R. China*

Abstract In this paper, we present a class of novel Bernstein-like basis functions, which is an extension of classical Bernstein basis functions. The properties of this group of bases are analyzed and the Bézier-like curve with two shape parameters h_1, h_2 is defined. The basis functions and Bézier-like curves have properties similar to cubic Bernstein basis functions and cubic Bézier curves, respectively. Furthermore, we construct Bézier-like curves with energy constraints and consider the C^1 and G^1 Hermite interpolation with minimal energy. Finally, some representative examples show the applicability and effectiveness of the proposed method.

Keywords Bézier-like curve; Hermite interpolation; Internal energy

MR(2020) Subject Classification 65D17; 65D18

1. Introduction

Bézier curves and surfaces are not only widely used modelling tools in CAD/CAM systems, but also powerful tools for shape design and geometric representation [1]. They are constructed by Bernstein basis functions, which have many beneficial properties. In recent years, in order to adjust the shape or change the position of a curve or surface so that it has better shape adjustability and approximation, scholars put forward various Bézier curves and surfaces with shape parameters, and correspondingly generalized various forms of Bézier curves and surfaces. Han et al. [2] analyzed the shape features of T-Bézier curves with a shape parameter by using the theory of envelop and topological mapping. Yan and Liang [3] proposed a novel kind of Bernstein-like basis by a recursive approach, and then defined corresponding Bézier-like curves and surfaces, as well as B-B surfaces over the triangular domain. In addition, a new basis called the C-Bézier basis was proposed in [4] to construct the C-Bézier curves by using an integral approach. To solve the problems of shape adjustment and shape control of developable surfaces, two direct explicit methods were proposed in [5] for the computer-aided design of developable Bézier-like surfaces with multiple shape parameters.

Because of its geometric and physical significance, the construction of Bézier curves and surfaces satisfying certain constraints has important theoretical significance and application value

Received May 18, 2023; Accepted November 16, 2023
Supported by the National Natural Science Foundation of China (Grant No. 11801225) and University Science Research Project of Jiangsu Province (Grant No. 18KJB110005).
* Corresponding author
E-mail address: yongxiahaoujs@ujs.edu.cn (Yongxia HAO)

in CAGD. The geometric construction of curves with minimal energy has always been one of the important research topics, and there have been many studies on it. Xu et al. [6] pointed out three geometric constructions of Bézier curves with minimal internal energy. Monterde [7] solved the Plateau-Bézier problem in the case of tensor product Bézier surface with the Dirichlet energy instead of the area functional. Ahn et al. [8] gave a geometric construction method of quadratic Bézier curves under the constraints of minimum arc length and bending energy, and studied the transition problems of related circles. Furthermore, geometric Hermite interpolation is a natural generalization which deals with interpolation of geometric quantities such as points, tangent directions, curvatures, and so on. Lu [9] presented a novel method for quintic G^2 Hermite interpolation by minimizing the approximate strain energy. In order to obtain shape-preserving interpolation desired for applications, they also presented cubic G^1 Hermite interpolation in [10] by minimizing curvature variation energy subject to a feasible region. Actually, the C^1 Hermite interpolation has been applied to many fields in recent years, such as modeling scientific data [11], reconstruction of the river beds [12], and so on. Li [13] constructed the plane C^1 cubic Hermite interpolation curve by minimizing approximate strain energy, approximate curvature change energy and their combination forms.

The broad aim of this work is to develop a novel Bézier-like curve with Bernstein-like basis functions which associate with the parameters h_1, h_2. We construct the Bézier-like curve with h_1 and h_2 obtained by minimizing the internal energy with an algorithm based on block coordinate descend (BCD) and proximal gradient method (PGM) in the feasible region. This enables us to generate Bézier-like curves with a wide variety of desired properties. Furthermore, we discuss the construction of Bézier-like curves with Hermite interpolation by minimizing the energy constraints.

The paper is organized as follows. In Section 2, we present the related definitions and properties of Bernstein-like basis functions and Bézier-like curves. In Section 3, we introduce several commonly used energy functionals and study the optimization problem to construct the Bézier-like curves with minimal internal energy. Moreover, the algorithm based on the BCD and PGM is presented, and various examples and applications are given to show the efficiency of the method. Finally, we present a conclusion in Section 4.

2. Bézier-like curves with shape parameters

In this section, we introduce the Bernstein-like basis functions and corresponding Bézier-like curves.

2.1. Definition of basis functions

Firstly, we present the definition of Bernstein-like basis functions.

Definition 2.1 *Let $h_1 \in [1, 4]$, $h_2 \in [0, 3]$, for any $t \in [0, 1]$, the following functions with respect*

to t

$$\begin{cases} F_0^3(t) = (h_1-3)t^4 + (8-3h_1)t^3 + (3h_1-6)t^2 - h_1 t + 1; \\ F_1^3(t) = h_1 t^3 - 2h_1 t^2 + h_1 t; \\ F_2^3(t) = (h_2 - h_1 + 2)t^4 + (2h_1 - h_2 - 8)t^3 + (6-h_1)t^2; \\ F_3^3(t) = (1-h_2)t^4 + h_2 t^3, \end{cases} \tag{2.1}$$

are called the Bernstein-like basis functions associated with the shape parameters h_1, h_2.

It is obvious that the Bernstein-like basis functions have the following properties:

(1) Degeneracy. When the parameters $h_1 = 3$, $h_2 = 1$, the Bernstein-like basis functions happen to be the traditional cubic Bernsterin basis functions.

(2) Partition of unity. The basis functions have $\sum_{i=0}^{3} F_i^3(t) = 1$.

(3) Non-negativity. After simplification, the basis functions have

$$\begin{cases} F_0^3(t) = -(t-1)^3((3-h_1)t+1); \\ F_1^3(t) = (t-1)^2 h_1 t; \\ F_2^3(t) = t^2(t-1)(h_1(1-t) + (2+h_2)t - 6); \\ F_3^3(t) = t^3(h_2(1-t) + t). \end{cases}$$

Clearly, for any $t \in [0,1]$, $h_1 \in [1,4]$ and $h_2 \in [0,3]$,

$$\begin{cases} (3-h_1)t + 1 \geq -t + 1 \geq 0; \\ (t-1)^2 h_1 t \geq 0; \\ h_1(1-t) + (2+h_2)t - 6 \leq 4(1-t) + 5t - 6 \leq 0; \\ h_2(1-t) + t \geq 0, \end{cases}$$

thus $F_i^3(t) \geq 0, i = 0,1,2,3$ for any $h_1 \in [1,4]$, $h_2 \in [0,3]$.

(4) Terminal Properties. $F_0^3(0) = 1$, $F_i^3(0) = 0$, $i = 1,2,3$; $F_3^3(1) = 1$, $F_i^3(1) = 0$, $i = 0,1,2$.

(5) Linear independence. For any $h_1 \in [1,4]$, $h_2 \in [0,3]$, the basis functions $F_i^3(t)$, $i = 0,1,2,3$ are linearly independent.

2.2. Construction of Bézier-like curves

By the Bernstein-like basis functions, we can construction the Bézier-like curves.

Definition 2.2. *Given four control points* $\boldsymbol{P}_i \in \mathbb{R}^n$ $(n = 2,3; i = 0,1,2,3)$, *the curves*

$$\boldsymbol{P}(t; h_1, h_2) = \sum_{i=0}^{3} F_i^3(t)\boldsymbol{P}_i, \quad t \in [0,1] \tag{2.2}$$

are called the Bézier-like curves with shape parameters h_1, h_2, *where* $h_1 \in [1,4]$, $h_2 \in [0,3]$.

The Eq. (2.2) can be rewritten into matrix form as

$$\mathbf{P}(t; h_1, h_2) = THQ, \tag{2.3}$$

where

$$T=\left[\begin{array}{cccccc} 1, & t, & t^2, & t^3, & t^4 \end{array}\right], \ Q=\left[\begin{array}{cccccc} \mathbf{P}_0, & \mathbf{P}_1, & \mathbf{P}_2, & \mathbf{P}_3 \end{array}\right]^{\mathrm{T}},$$

$$H=\left[\begin{array}{cccc} 1 & 0 & 0 & 0 \\ -h_1 & h_1 & 0 & 0 \\ 3h_1-6 & -2h_1 & 6-h_1 & 0 \\ 8-3h_1 & h_1 & 2h_1-h_2-8 & h_2 \\ h_1-3 & 0 & h_2-h_1+2 & 1-h_2 \end{array}\right].$$

Obviously, when $h_1=3$, $h_2=1$, the Eq. (2.3) becomes the matrix expression of cubic Bézier curves. It also shows that the Bézier-like curves with shape parameters h_1, h_2 is an extension of cubic Bézier curve.

From the properties of the basis functions (2.1), the Bézier-like curves with shape parameters have the following properties:

(1) End-points properties. For any $h_1 \in [1,4]$, $h_2 \in [0,3]$, we have

$$\mathbf{P}(0;h_1,h_2)=\mathbf{P}_0, \quad \mathbf{P}(1;h_1,h_2)=\mathbf{P}_3.$$

Furthermore, the derivatives at end-points satisfy

$$\mathbf{P}'(0;h_1,h_2)=h_1(\mathbf{P}_1-\mathbf{P}_0), \quad \mathbf{P}'(1;h_1,h_2)=(h_2-4)(\mathbf{P}_2-\mathbf{P}_3).$$

Similarly, we also have the second derivative at end-points

$$\mathbf{P}''(0;h_1,h_2)=2h_1(3\mathbf{P}_0-\mathbf{P}_2-2\mathbf{P}_1)+12(\mathbf{P}_2-\mathbf{P}_0),$$
$$\mathbf{P}''(1;h_1,h_2)=2h_1(\mathbf{P}_1-\mathbf{P}_2)+(12-6h_2)(\mathbf{P}_3-\mathbf{P}_2).$$

(2) Convex hull property. From the partition of unity and the non-negativity of the basis functions, the entire parametric curves must lie inside the convex hull of the control polygon spanned by $\mathbf{P}_0$, $\mathbf{P}_1$, $\mathbf{P}_2$, $\mathbf{P}_3$.

(3) Geometric invariability and affine invariance. Eq. (2.3) is a vector function, so the shape of the parametric curve is only related to the control points, and it is independent of the selection of coordinates, which means (2.3) satisfies the following two equations:

$$\mathbf{P}(t;h_1,h_2;\mathbf{P}_0+\mathbf{C},\mathbf{P}_1+\mathbf{C},\mathbf{P}_2+\mathbf{C},\mathbf{P}_3+\mathbf{C})=\mathbf{P}(t;h_1,h_2;\mathbf{P}_0,\mathbf{P}_1,\mathbf{P}_2,\mathbf{P}_3)+\mathbf{C},$$
$$\mathbf{P}(t;h_1,h_2;\mathbf{MP}_0,\mathbf{MP}_1,\mathbf{MP}_2,\mathbf{MP}_3)=\mathbf{MP}(t;h_1,h_2;\mathbf{P}_0,\mathbf{P}_1,\mathbf{P}_2,\mathbf{P}_3),$$

where $\mathbf{C}$ is an arbitrary vector in $\mathbb{R}^2$ or $\mathbb{R}^3$ and $\mathbf{M}$ is an arbitrary $l\times l$ matrix, $l=2$ or 3.

(4) Variation diminishing property. Since the Bernstein-like basis functions given in (2.1) are a group of normalized totally positive basis functions, the Bézier-like curves in (2.2) has the property of diminishing variation. That is, the number of intersections of a Bézier-like curve with any line in the same plane will be no more than the number of intersections of its control polygon with the line.

(5) Shape adjustable property. Due to the shape parameters h_1, h_2, the curves become more adjustable. When the control points remain unchanged, by changing the shape parameters h_1, h_2, a group of curves with different shapes will be obtained, which is very convenient for the

design of free curves. Figure 1 presents an illustration of the shape adjustable property. Given $\mathbf{P}_0 = (0,0)$, $\mathbf{P}_1 = (\frac{1}{3}, \frac{1}{3})$, $\mathbf{P}_2 = (\frac{2}{3}, \frac{1}{3})$ and $\mathbf{P}_3 = (1,0)$, fixing one parameter of h_1 and h_2 and changing the other one, a group of curves with different shapes are obtained.

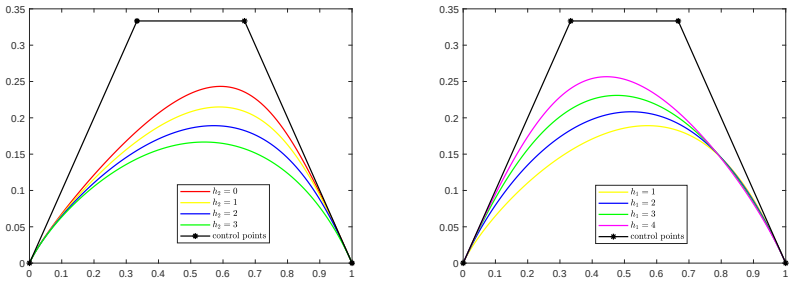

(a) $h_1 = 1$ (b) $h_2 = 2$

Figure 1 Shape adjustable property

3. Construction of Bézier-like curves with internal energy

In this section, we study the construction of Bézier-like curves with different internal energy. We briefly introduce the commonly used internal energy functions, and explain in detail the problems we need to study.

3.1. Internal energy of curves

The internal energy and external energy of a curve are collectively referred to as the total energy of the curve [14]. Internal energy refers to the energy that depends on the internal properties of the curve, such as tangent vector and curvature, etc.

In this section, we will introduce three commonly used energy functions. Bending energy is the most widely used internal energy of a curve, for any parametric curve $\mathbf{x}(t)$, $t \in [a,b]$, the bending energy is

$$E_{\text{bend}}(\mathbf{x}) = \int_a^b k^2(t)\|\mathbf{x}'(t)\|\mathrm{d}t, \tag{3.1}$$

where $k(t)$ is the curvature of the curve. The history of bending energy can be traced back to the work of Bernoulli et al. [15] in the 18th century. It is known from experience that such energy can yield smooth curves, which seems to be an appropriate choice. Since

$$\int_a^b k^2(t)\|\mathbf{x}'(t)\|\mathrm{d}t = \int_a^b \frac{\|\mathbf{x}'(t) \times \mathbf{x}''(t)\|^2}{\|\mathbf{x}'(t)\|^5}\mathrm{d}t,$$

when the curve has a nearly arc length parametrization $\mathbf{x}'(t) \doteq 1$, the following approximation is widely used:

$$\int_a^b \|\mathbf{x}''(t)\|^2\mathrm{d}t.$$

In some cases the bending energy can be reduced by introducing large loops, in order to avoid this undesirable situation, the length of the curve must be restricted. A common method is to

combine bending energy with another functional, which is the length of the curve. Because this functional makes the curve stretching, it is called stretch energy:

$$E_{\text{stretch}}(\mathbf{x}) = \int_a^b \|\mathbf{x}'(t)\|\mathrm{d}t. \tag{3.2}$$

From Schwarz inequality,

$$\Big(\int_a^b \|\mathbf{x}'(t)\|\mathrm{d}t\Big)^2 \le (b-a)\int_a^b \|\mathbf{x}'(t)\|^2\mathrm{d}t,$$

it means

$$E^2_{\text{stretch}}(\mathbf{x}) \le (b-a)\int_a^b \|\mathbf{x}'(t)\|^2\mathrm{d}t,$$

so the following approximation is often used instead:

$$\int_a^b \|\mathbf{x}'(t)\|^2\mathrm{d}t.$$

For 3D curves, torsion describes the total amount of twisting (planar curves have zero torsion). The degree of distortion can be reduced by twisting energy

$$E_{\text{twist}}(\mathbf{x}) = \int_a^b \tau^2(t)\|\mathbf{x}'(t)\|\mathrm{d}t, \tag{3.3}$$

where τ is the torsion of the curve. Constrain the twist energy so that the curve does not deviate from the plane at each point, making the curve as flat as possible [14]. If estimating or minimizing the Eqs. (3.1)–(3.3) directly, it would make the computation too complicated. Therefore, the following energy functions are generally used instead:

$$E_1(\mathbf{x}) = \int_a^b \|\mathbf{x}'(t)\|^2\mathrm{d}t, \tag{3.4}$$

$$E_2(\mathbf{x}) = \int_a^b \|\mathbf{x}''(t)\|^2\mathrm{d}t, \tag{3.5}$$

$$E_3(\mathbf{x}) = \int_a^b \|\mathbf{x}'''(t)\|^2\mathrm{d}t, \tag{3.6}$$

for approximate estimation [14]. The advantage of these approximations is that, for example, for B-spline curves, they are quadratic functions of control points. This is probably the reason for their popularity, since quadratic functions can be efficiently minimized. A disadvantage of the approximations (3.4)–(3.6) is that they are parameterization dependent.

3.2. Bézier-like curves with minimal internal energy

In this section, our goal is to construct the Bézier-like curves by minimizing the internal energy functions (3.4)–(3.6), respectively.

Given the control points $\{\mathbf{P}_i\}_{i=0}^3$, we can get the corresponding constrained optimization problem:

$$\min_{(h_1,h_2)\in D} E_i(\mathbf{P}; h_1, h_2), \quad i = 1, 2, 3, \tag{3.7}$$

where $D = [1,4] \times [0,3]$, for the Bézier-like curve

$$\mathbf{P}(t;h_1,h_2) = \sum_{i=0}^{3} F_i^3(t)\mathbf{P}_i, \quad t \in [0,1].$$

For the convenience of calculation, we give the matrix representation of energy. The purpose is to convert the integral of Bernstein-like basis function product to the integral of power basis product, so as to reduce the computational complexity. From the Eq. (2.3), we have

$$\mathbf{P}'(t;h_1,h_2) = [1,t,t^2,t^3]M_1Q, \quad \mathbf{P}''(t;h_1,h_2) = [1,t,t^2]M_2Q, \quad \mathbf{P}'''(t;h_1,h_2) = [1,t]M_3Q,$$

where

$$M_1 = \begin{bmatrix} -h_1 & h_1 & 0 & 0 \\ 2(3h_1-6) & -4h_1 & 2(6-h_1) & 0 \\ 3(8-3h_1) & 3h_1 & 3(2h_1-h_2-8) & 3h_2 \\ 4(h_1-3) & 0 & 4(h_2-h_1+2) & 4(1-h_2) \end{bmatrix},$$

$$M_2 = \begin{bmatrix} 2(3h_1-6) & -4h_1 & 2(6-h_1) & 0 \\ 6(8-3h_1) & 6h_1 & 6(2h_1-h_2-8) & 6h_2 \\ 12(h_1-3) & 0 & 12(h_2-h_1+2) & 12(1-h_2) \end{bmatrix},$$

$$M_3 = \begin{bmatrix} 6(8-3h_1) & 6h_1 & 6(2h_1-h_2-8) & 6h_2 \\ 24(h_1-3) & 0 & 24(h_2-h_1+2) & 24(1-h_2) \end{bmatrix},$$

$$Q = \begin{bmatrix} \mathbf{P}_0, & \mathbf{P}_1, & \mathbf{P}_2, & \mathbf{P}_3 \end{bmatrix}^{\mathrm{T}}.$$

Then we can obtain

$$E_1(\mathbf{P};h_1,h_2) = \int_0^1 \|\mathbf{P}'(t)\|^2 \mathrm{d}t = \frac{1}{70}Q^{\mathrm{T}}M_1^{\mathrm{T}} \int_0^1 \begin{bmatrix} 1 & t & t^2 & t^3 \\ t & t^2 & t^3 & t^4 \\ t^2 & t^3 & t^4 & t^5 \\ t^3 & t^4 & t^5 & t^6 \end{bmatrix} \mathrm{d}t M_1 Q = \frac{1}{70}Q^{\mathrm{T}}MQ,$$

where

$$M = \begin{bmatrix} M_{00} & M_{01} & M_{02} & M_{03} \\ M_{01} & M_{11} & M_{12} & M_{13} \\ M_{02} & M_{12} & M_{22} & M_{23} \\ M_{03} & M_{13} & M_{23} & M_{33} \end{bmatrix},$$

$$M_{00} = 6h_1^2 - 8h_1 + 96, \ M_{01} = -7{h_1}^2, \ M_{02} = h_1^2 + (2-h_2)h_1 + 10h_2 - 64,$$

$$M_{03} = (h_2+6)h_1 - 10h_2 - 32, \ M_{11} = \frac{28h_1^2}{3}, \ M_{12} = \frac{7h_1(6-h_1)}{3},$$

$$M_{13} = -14h_1, \ M_{22} = \frac{4h_1}{3}(h_1+2h_2-24) + 6h_2(h_2-10) + 192,$$

$$M_{23} = 8h_1 + 50h_2 - h_1h_2 - 6h_2^2 - 128, \ M_{33} = 6h_2^2 - 40h_2 + 160.$$

Similarly, for the energy E_2, E_3, we have

$$E_2(\mathbf{P};h_1,h_2) = \frac{1}{5}Q^{\mathrm{T}}NQ, \quad E_3(\mathbf{P};h_1,h_2) = 12Q^{\mathrm{T}}OQ,$$

where

$$N = \begin{bmatrix} N_{00} & N_{01} & N_{02} & N_{03} \\ N_{01} & N_{11} & N_{12} & N_{13} \\ N_{02} & N_{12} & N_{22} & N_{23} \\ N_{03} & N_{13} & N_{23} & N_{33} \end{bmatrix}, \quad O = \begin{bmatrix} O_{00} & O_{01} & O_{02} & O_{03} \\ O_{01} & O_{11} & O_{12} & O_{13} \\ O_{02} & O_{12} & O_{22} & O_{23} \\ O_{03} & O_{13} & O_{23} & O_{33} \end{bmatrix}$$

and

$$\begin{aligned} &N_{00} = 24h_1^2 - 84h_1 + 96, \quad N_{01} = -20h_1^2 + 30h_1, \quad N_{02} = -4h_1^2 + (60 - 6h_2)h_1 + 18h_2 - 144, \\ &N_{03} = (6h_2 - 6)h_1 + 48 - 18h_2, \quad N_{11} = 20h_1^2, \quad N_{12} = (10h_2 - 40)h_1, \quad N_{13} = (10 - 10h_2)h_1, \\ &N_{22} = 4h_1^2 + (-8h_2 - 16)h_1 + 24h_2^2 - 144h_2 + 336, \quad N_{23} = 126h_2 - 4h_1 + 4h_1h_2 - 24h_2^2 - 192, \\ &N_{33} = 24h_2^2 - 108h_2 + 144 \end{aligned}$$

and

$$\begin{aligned} &O_{00} = 7h_1^2 - 36h_1 + 48, \quad O_{01} = -3h_1(h_1 - 2), \quad O_{02} = (h_1 - 6)(h_2 - 4h_1 + 8), \\ &O_{03} = (-h_2 - 2)h_1 + 6h_2, \quad O_{11} = 3h_1^2, \quad O_{12} = (3h_2 - 12)h_1, \quad O_{13} = 3h_1(h_2 - 2), \\ &O_{22} = 4h_1^2 - 8h_1h_2 - 16h_1 + 7h_2^2 - 8h_2 + 64, \quad O_{23} = (4h_2 - 4)h_1 - 7h_2^2 + 14h_2 - 16, \\ &O_{33} = 7h_2^2 - 20h_2 + 16. \end{aligned}$$

At first glance, it is natural to determine h_1 and h_2 through taking the derivative of h_1, h_2, however, as a result of the parameters $h_1 \in [1, 4]$, $h_2 \in [0, 3]$, we cannot solve the problem (3.7) by taking the derivative directly. Several algorithms have been proposed to solve the minimization problem. Lu [10] proposed a numerical iterative approach based on the block coordinate descend (BCD) method [16, 17]. The BCD method is derivative-free, and at each iteration, finds the optimal value of one coordinate while the other coordinates remain fixed; hence, it is particularly suitable for solving optimization problems with only a few unknowns. In [9], the algorithm based on the proximal gradient method (PGM) was presented. Here we put forward a novel algorithm based on PGM and BCD to solve the minimization problem (3.7). The entire algorithm to find the optimal solution for (h_1, h_2) is described in Algorithm 1.

In Line 1, we choose an initial guess for h_1 and h_2 in the feasible region. In Line 3, we fix the value of h_2 as the value obtained in the previous step, and then we can get the gradient by h_1. In Line 4, we optimize the step length by the so-called line search method. In Line 5, we project the new point $\mathbf{x}$ orthogonally to the nearest point in D by proximal mapping to obtain the h_1:

$$\Pi_D(\mathbf{x}) = \begin{cases} \mathbf{x}, & \text{if } \mathbf{x} \in D, \\ \arg\min\limits_{\mathbf{z} \in D} ||\mathbf{z} - \mathbf{x}||^2, & \text{otherwise.} \end{cases} \tag{3.8}$$

Algorithm 1: Finding the optimal solution for (h_1, h_2) by E_i.

1: Choose an initial value for (h_1^0, h_2^0), and set $k = 0$;

2: **repeat**

3: Fix $h_2 = h_2^k$ in $E_i(h_1, h_2)$, then compute the gradient of h_1, $\nabla E_i := \nabla E_i(h_1, h_2^k)$; take $h_1 = h_1^k$ in ∇E_i, obtain ∇E_i^k;

4: Find the locally optimal step length: $s_k = \arg\min_s E_i(h_1^k - s\nabla E_i^k, h_2^k)$;

5: Compute $h_1^{k+1} = \Pi_D(h_1^k - s_k \nabla E_i^k)$;

6: Fix $h_1 = h_1^{k+1}$ in $E_i(h_1, h_2)$ $(i = 1, 2, 3)$, then compute the gradient of h_2 $\nabla \hat{E}_i := \nabla \hat{E}_i(h_1^{k+1}, h_2)$; take $h_2 = h_2^k$ in $\nabla \hat{E}_i$, obtain $\nabla \hat{E}_i^k$;

7: Find the locally optimal step length: $t_k = \arg\min_t \hat{E}_i(h_1^{k+1}; h_2^k - t\nabla \hat{E}_i^k)$;

8: Compute $h_2^{k+1} = \Pi_D(h_2^k - t_k \nabla \hat{E}_i^k)$;

9: $k = k + 1$;

10: **until** $|h_1^{k+1} - h_1^k| + |h_2^{k+1} - h_2^k| < \epsilon$;

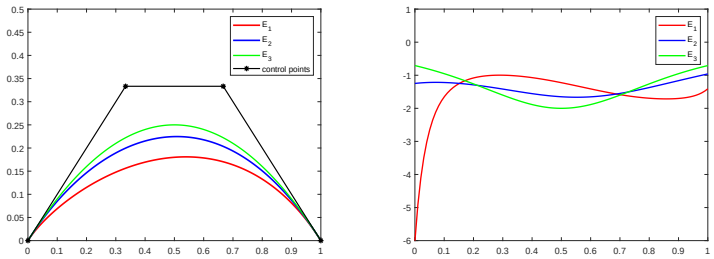

(a) $\mathbf{P}_0 = (0, 0)$, $\mathbf{P}_1 = (\frac{1}{3}, \frac{1}{3})$, $\mathbf{P}_2 = (\frac{2}{3}, \frac{1}{3})$, $\mathbf{P}_3 = (1, 0)$

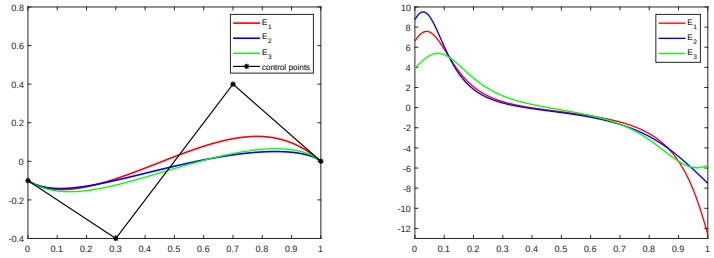

(b) $\mathbf{P}_0 = (0, 0)$, $\mathbf{P}_1 = (\frac{3}{10}, -\frac{2}{5})$, $\mathbf{P}_2 = (\frac{7}{10}, \frac{2}{5})$, $\mathbf{P}_3 = (1, 0)$

Figure 2 Example 3.1

According to the result in references [16,17], this algorithm only requires the initial value to be selected within the feasible domain, so the order of h_1 and h_2 and the initial value selection

do not affect the result. In the following examples, the initial value of (h_1, h_2) is usually taken as the central point of feasible region D, and the threshold value for the algorithm is $\epsilon = 1 \times 10^{-7}$.

Example 3.1 In this example, given two groups of control points, construct the Bézier-like curves with minimal energy E_1, E_2 and E_3, respectively. In Figure 2 (a), C-shaped Bézier-like curves are obtained by minimizing internal energy E_i $(i = 1, 2, 3)$ respectively, while in Figure 2 (b), S-shaped curves are displayed. Moreover, the corresponding curvature plots are also presented. Table 1 lists the comparison of different energy values and the curvature informations of the Bézier-like curves. Here the average curvature (AC) is defined as the average value of the curvature of 500 points selected from the curve. Since the curvature varies where there are high changes of the tangent vector, but where the curve is flat it is almost constant, so the curvature plot is used to reflect the flatness of the curves under different energy minimization.

Energy	(h_1, h_2)	E_1	E_2	E_3	AC
E_1(3.1(a))	(1.2889,2.6074)	1.2227	5.7462	120.39	-1.5518
E_2(3.1(a))	(2.4553,1.6704)	1.2674	3.1899	14.78	-1.3954
E_3(3.1(a))	(3.0000,1.0000)	1.3333	4.0000	0	-1.4071
E_1(3.1(b))	(1.9382,3.0000)	1.1509	9.3466	166.2115	-0.4036
E_2(3.1(b))	(1.7609,2.7750)	1.1545	9.2618	170.41	-0.1141
E_3(3.1(b))	(2.4173,2.3597)	1.1703	10.374	145.86	-0.2329

Table 1 Comparison of different curves in Figure 2

3.3. C^1 Bézier-like curves with minimal internal energy

In this section, we aim to find a C^1 Hermite interpolation Bézier-like curve with minimal internal energy.

Given C^1 Hermite data $\{\mathbf{P}_0, \mathbf{P}_3, \mathbf{T}_0, \mathbf{T}_1\}$ represented by the positions and tangents at two end points, a C^1 Bézier-like curve is

$$\mathbf{P}(t; h_1, h_2) = \sum_{i=0}^{3} F_i^3(t)\mathbf{P}_i, \quad t \in [0, 1]$$

with $\mathbf{P}_1, \mathbf{P}_2$ expressed as

$$\mathbf{P}_1 = \frac{\mathbf{T}_0}{h_1} + \mathbf{P}_0, \quad \mathbf{P}_2 = \mathbf{P}_3 + \frac{\mathbf{T}_1}{h_2 - 4},$$

where $(h_1, h_2) \in D = [1, 4] \times [0, 3]$.

Similarly, in order to reduce the computational complexity, the matrix representations of the energy E_i $(i = 1, 2, 3)$ are presented as follows:

$$\tilde{E}_1(\mathbf{P}; h_1, h_2) = \int_0^1 \|\mathbf{P}'(t)\|^2 \mathrm{d}t = \frac{1}{210} R^{\mathrm{T}} U R,$$

$$\tilde{E}_2(\mathbf{P}; h_1, h_2) = \frac{1}{5} R^{\mathrm{T}} V R, \quad \tilde{E}_3(\mathbf{P}; h_1, h_2) = 12 R^{\mathrm{T}} W R,$$

where

$$U=\begin{bmatrix} U_{00} & U_{01} & U_{02} & U_{03}\\ U_{01} & U_{11} & U_{12} & U_{13}\\ U_{02} & U_{12} & U_{22} & U_{23}\\ U_{03} & U_{13} & U_{23} & U_{33}\end{bmatrix},\quad R=\begin{bmatrix}\mathbf{P}_0, & \mathbf{P}_3, & \mathbf{T}_0, & \mathbf{T}_1\end{bmatrix}^{\mathrm{T}},$$

$$V=\begin{bmatrix} V_{00} & V_{01} & V_{02} & V_{03}\\ V_{01} & V_{11} & V_{12} & V_{13}\\ V_{02} & V_{12} & V_{22} & V_{23}\\ V_{03} & V_{13} & V_{23} & V_{33}\end{bmatrix},\quad W=\begin{bmatrix} W_{00} & W_{01} & W_{02} & W_{03}\\ W_{01} & W_{11} & W_{12} & W_{13}\\ W_{02} & W_{12} & W_{22} & W_{23}\\ W_{03} & W_{13} & W_{23} & W_{33}\end{bmatrix},$$

$$U_{00}=4(h_1^2-6h_1+72),\ U_{01}=-4(h_1^2-6h_1+72),\ U_{02}=7h_1,$$
$$U_{03}=-\frac{3h_1(h_2-48+4h_1)-30h_2+192}{h_2-4},\ U_{11}=4(h_1^2-6h_1+72),\ U_{12}=-7h_1,$$
$$U_{13}=\frac{3h_1(h_2-48+4h_1)-30h_2+192}{h_2-4},\ U_{22}=28,\ U_{23}=-\frac{7(h_1-6)}{(h_2-4)},$$
$$U_{33}=\frac{2(2h_1^2+3h_1(h_2-12)+9h_2(h_2-10)+288)}{(h_2-4)^2}.$$

$$V_{00}=4h_1^2-24h_1+96,\ V_{01}=-(4h_1^2-24h_1+96),\ V_{02}=30,$$
$$V_{03}=\frac{4(5h_1+h_1h_2-h_1^2)+18h_2-144}{h_2-4},\ V_{11}=4(h_1^2-6h_1+24),\ V_{12}=-30,$$
$$V_{13}=-\frac{4(5h_1+h_1h_2-h_1^2)+18h_2-144}{h_2-4},\ V_{22}=20,\ V_{23}=10,$$
$$V_{33}=\frac{4(-h_1^2+2h_1h_2+4h_1-6h_2^2+36h_2-84)}{(h_2-4)^2}$$

and

$$W_{00}=4(h_1^2-6h_1+12),\ W_{01}=-4(h_1^2-6h_1+12),\ W_{02}=72,$$
$$W_{03}=-\frac{2(3h_2-10h_1-2h_1h_2+2h_1^2+24)}{h_2-4},\ W_{11}=-4(h_1^2-6h_1+12),\ W_{12}=-72,$$
$$W_{13}=\frac{2(3h_2-10h_1-2h_1h_2+2h_1^2+24)}{h_2-4},\ W_{22}=3,\quad W_{23}=3,$$
$$W_{33}=-\frac{-4h_1^2+8h_1h_2+16h_1-7h_2^2+8h_2-64}{(h_2-4)^2}.$$

Since h_1 and h_2 take values in D, we can also use Algorithm 1 to solve the minimization problem:

$$\min_{(h_1,h_2)\in D}\tilde{E}_i(h_1,h_2),\quad i=1,2,3. \tag{3.9}$$

Theorem 3.2 *The minimum point of $\tilde{E}_2(h_1,h_2)$ and $\tilde{E}_3(h_1,h_2)$ is $(h_1,h_2)=(3,1)$.*

Proof It can be easily checked that

$$\tilde{E}_2(h_1,h_2)-\tilde{E}_2(3,1)=\frac{4[(h_2-h_1+2)\mathbf{T}_1+(h_1h_2-3h_2-4h_1+12)(\mathbf{P}_0-\mathbf{P}_3)]^2}{5(h_2-4)^2}.$$

Obviously, $\tilde{E}_2(h_1,h_2)-\tilde{E}_2(3,1)\geq 0$. Hence $(h_1,h_2)=(3,1)$ is the minimum point of $\tilde{E}_2$. Similarly, from

$$\tilde{E}_3(h_1,h_2)-\tilde{E}_3(3,1)=\frac{48[(h_2-h_1+2)\mathbf{T}_1+(h_1h_2-3h_2-4h_1+12)(\mathbf{P}_0-\mathbf{P}_3)]^2}{(h_2-4)^2},$$

we have $\tilde{E}_3(h_1,h_2)\geq\tilde{E}_3(3,1)$, so $(h_1,h_2)=(3,1)$ is also the minimum point of $\tilde{E}_3$. □

Example 3.3 Similarly as Example 3.1, Figure 3 illustrates two representative examples for a comparison of C^1 Bézier-like curves. By Theorem 3.2, the C^1 Bézier-like curves with minimal $\tilde{E}_2$ or $\tilde{E}_3$ energy is just the cubic C^1 Bézier curve with $h_1=3,h_2=1$. Therefore, Figure 3 compares the C^1 Bézier-like curves with minimal $\tilde{E}_1$ and $\tilde{E}_2$ energy respectively. Given the control points $\mathbf{P}_0$, $\mathbf{P}_1$ and tangent vectors $\mathbf{T}_0$, $\mathbf{T}_1$, the parameters h_1 and h_2 can be obtained by Algorithm 1. The comparative energies and curvature information are listed in Table 2.

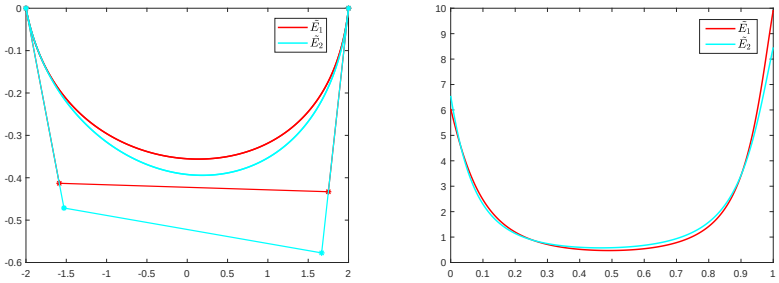

(a) $\mathbf{P}_0=(-2,0)$, $\mathbf{P}_3=(2,0)$, $\mathbf{T}_0=2(\cos(-\frac{\pi}{4}),\sin(-\frac{\pi}{4}))$, $\mathbf{T}_1=2(\cos\frac{\pi}{3},\sin\frac{\pi}{3})$

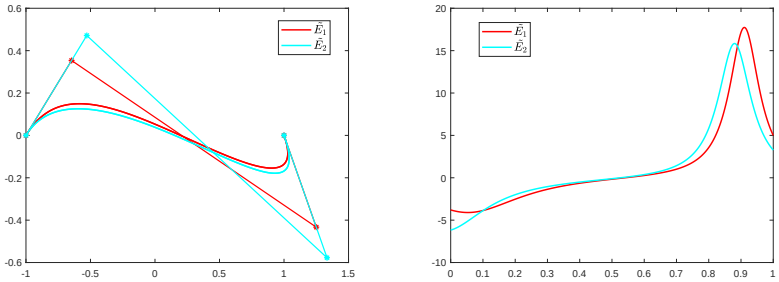

(b) $\mathbf{P}_0=(-1,0)$, $\mathbf{P}_3=(1,0)$, $\mathbf{T}_0=2(\cos\frac{\pi}{4},\sin\frac{\pi}{4})$, $\mathbf{T}_1=-2(\cos(-\frac{\pi}{3}),\sin(-\frac{\pi}{3}))$

Figure 3 Example 3.3

Energy	h_1	h_2	$\tilde{E}_1$	$\tilde{E}_2$	$\tilde{E}_3$	AC
$\tilde{E}_1$(3.2(a))	3.4236	0	18.2794	105.7139	1231.1088	1.8449
$\tilde{E}_2$(3.2(a))	3	1	18.4043	103.9766	1126.8731	1.8440
$\tilde{E}_1$(3.2(b))	4	0	5.3446	79.8000	1155.2464	1.3076
$\tilde{E}_2$(3.2(b))	3	1	5.6320	74.2000	819.2464	1.3035

Table 2 Comparison of different curves in Figure 3

Example 3.4 In order to make a comprehensive comparison, three representative examples are illustrated in Figure 4. Figure 4 (a) shows an S-shaped curve obtained by our C^1 method with minimal $\tilde{E}_1$ and $\tilde{E}_2$ energy respectively. Figure 4 (b) presents the C^1 approximations using three segments from a piece of Euler spiral expressed by

$$x(s) = \int_0^s \cos\frac{\pi}{2}t^2 \mathrm{d}t,\ y(s) = \int_0^s \sin\frac{\pi}{2}t^2 \mathrm{d}t, \quad s \in [0, 2].$$

Euler spirals, having linearly changing curvature, are widely regarded as a kind of fair curves in motion planning and railway design. The original Euler spiral curve, the joined C^1 interpolating Bézier-like curves and Bézier curves are displayed. Finally, we consider piecewise C^1 interpolants of a starfish curve expressed by

$$x(t) = (1 + \frac{1}{5}\cos(5t))\cos t,\ y(t) = (1 + \frac{1}{5}\cos(5t))\sin t, \quad t \in [0, 2]$$

with the data sampled at $t = \frac{i\pi}{5}$, $i = 0, \ldots, 9$. Obviously, our method can achieve good fitting effect with minimum energy.

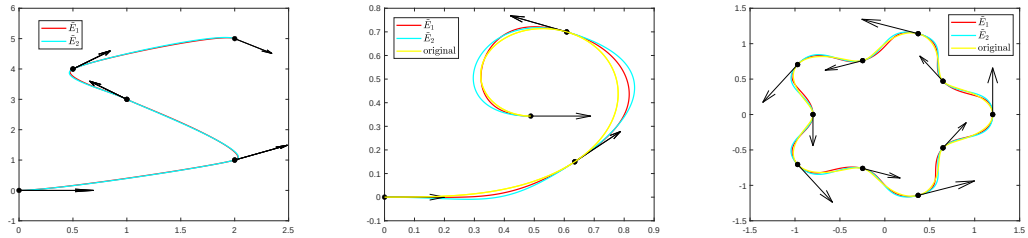

(a) S-shaped Bézier-like curve (b) Euler spiral (c) Starfish curve

Figure 4 Example 3.4

3.4. G^1 Bézier-like curves with minimal internal energy

In this section, we propose to construct a G^1 Hermite interpolation Bézier-like curve with minimal internal energy.

Given G^1 Hermite data $\{\mathbf{P}_0, \mathbf{P}_3, \mathbf{T}_0, \mathbf{T}_1\}$ represented by the positions and unit tangents at two end points, a cubic G^1 interpolating curve is

$$\mathbf{P}(t; h_1, h_2) = \sum_{i=0}^{3} F_i^3(t)\mathbf{P}_i, \quad t \in [0, 1]$$

with $\mathbf{P}_1, \mathbf{P}_2$ expressed as

$$\mathbf{P}_1 = \frac{\alpha\mathbf{T}_0}{h_1} + \mathbf{P}_0, \quad \mathbf{P}_2 = \frac{\beta\mathbf{T}_1}{h_2 - 4} + \mathbf{P}_3,$$

and α, β are real numbers.

The next task is to determine the four unknowns h_1, h_2, α and β. The unknowns α, β can be assigned to any values according to different application requirements while always satisfying the G^1 Hermite conditions, because no constraint is imposed on them. Meanwhile, h_1, h_2 can be

determined by minimizing the energy E_i $(i = 1, 2, 3)$. We also give the matrix representation of the energy as follows.

$$\widehat{E}_1(\mathbf{P}; h_1, h_2, \alpha, \beta) = \int_0^1 \|\mathbf{P}'(t)\|^2 \mathrm{d}t = \frac{1}{210} S^{\mathrm{T}} X S,$$

where

$$X = \begin{bmatrix} X_{00} & X_{01} & X_{02} & X_{03} \\ X_{01} & X_{11} & X_{12} & X_{13} \\ X_{12} & X_{12} & X_{22} & X_{23} \\ X_{03} & X_{13} & X_{23} & X_{33} \end{bmatrix}, \quad S = \begin{bmatrix} \mathbf{P}_0, & \mathbf{P}_3, & \mathbf{T}_0, & \mathbf{T}_1 \end{bmatrix}^{\mathrm{T}}$$

with

$$\begin{aligned}
&X_{00} = 4(h_1^2 - 6h_1 + 72),\ X_{01} = -4(h_1^2 - 6h_1 + 72),\ X_{02} = 7\alpha h_1, \\
&X_{03} = \frac{-\alpha(3h_1(h_2 - 48 + 4h_1) - 30h_2 + 192)}{h_2 - 4},\ X_{11} = 4(h_1^2 - 6h_1 + 72),\ X_{12} = -7\alpha h_1, \\
&X_{13} = \frac{\beta(3h_1(h_2 - 48 + 4h_1) - 30h_2 + 192)}{h_2 - 4},\ X_{22} = 28\alpha^2, \\
&X_{23} = -\frac{7\alpha\beta(h_1 - 6)}{(h_2 - 4)},\ X_{33} = \frac{2\beta^2(2h_1^2 + 3h_1(h_2 - 12) + 9h_2(h_2 - 10) + 288)}{(h_2 - 4)^2}.
\end{aligned}$$

Similarly,

$$\widehat{E}_2(\mathbf{P}; h_1, h_2, \alpha, \beta) = \int_0^1 \|\mathbf{P}''(t)\|^2 \mathrm{d}t = \frac{1}{5} S^{\mathrm{T}} Y S,\ \widehat{E}_3(\mathbf{P}; h_1, h_2, \alpha, \beta) = \int_0^1 \|\mathbf{P}'''(t)\|^2 \mathrm{d}t = 12 S^{\mathrm{T}} Z S,$$

where

$$Y = \begin{bmatrix} Y_{00} & Y_{01} & Y_{02} & Y_{03} \\ Y_{01} & Y_{11} & Y_{12} & Y_{13} \\ Y_{12} & Y_{12} & Y_{22} & Y_{23} \\ Y_{03} & Y_{13} & Y_{23} & Y_{33} \end{bmatrix}, \quad Z = \begin{bmatrix} Z_{00} & Z_{01} & Z_{02} & Z_{03} \\ Z_{01} & Z_{11} & Z_{12} & Z_{13} \\ Z_{02} & Z_{12} & Z_{22} & Z_{23} \\ Z_{03} & Z_{13} & Z_{23} & Z_{33} \end{bmatrix}$$

and

$$\begin{aligned}
&Y_{00} = 4(h_1^2 - 6h_1 + 24),\ Y_{01} = -4(h_1^2 - 6h_1 + 24),\ Y_{02} = 30\alpha, \\
&Y_{03} = \frac{2\beta(h_1(-2h_1 + 2h_2 + 10) - 9h_2 - 72)}{h_2 - 4},\ Y_{11} = 4(h_1^2 - 6h_1 + 24),\ Y_{12} = -30\alpha, \\
&Y_{13} = \frac{-2\beta(h_1(-2h_1 + 2h_2 + 10) - 9h_2 - 72)}{h_2 - 4},\ Y_{22} = 20\alpha^2, \\
&Y_{23} = 2\alpha\beta,\ Y_{33} = \frac{-4\beta^2(-h_1^2 + 2h_1(h_2 + 2) + 6h_2(6 - h_2) - 84)}{(h_2 - 4)^2}
\end{aligned}$$

and

$$\begin{aligned}
&Z_{00} = 4(h_1^2 - 6h_1 + 24),\ Z_{01} = -4(h_1^2 - 6h_1 + 24),\ Z_{02} = 6\alpha, \\
&Z_{03} = \frac{-2\beta(2h_1(h_1 - h_2 - 5) + 3h_2 + 24)}{h_2 - 4},\ Z_{11} = 4(h_1^2 - 6h_1 + 24),\ Z_{12} = -6\alpha, \\
&Z_{13} = \frac{2\beta(2h_1(h_1 - h_2 - 5) + 3h_2 + 24)}{h_2 - 4},\ Z_{22} = 3\alpha^2,
\end{aligned}$$

$$Z_{23} = 3\alpha\beta,\ Z_{33} = \frac{-\beta^2(-4h_1^2 + 8h_1(h_2+2) + h_2(8-7h_2) - 64)}{(h_2-4)^2}.$$

It is natural to determine h_1, h_2, α_1 and β_1 through the following process:

$$\min_{h_1,h_2,\alpha,\beta} \widehat{E}_i(h_1, h_2, \alpha, \beta). \tag{3.10}$$

Since h_1 and h_2 are limited in a scope, in order to reduce the complexity of the problem, we can simplify $\widehat{E}_i$ to the function of h_1 and h_2. Taking $\widehat{E}_1$ as an example, by letting

$$\frac{\partial \widehat{E}_1}{\partial \alpha} = \frac{\partial \widehat{E}_1}{\partial \beta} = 0,$$

where

$$\begin{aligned}
\frac{\partial \widehat{E_1}}{\partial \alpha} =& \frac{4\alpha + 4h_1\langle \mathbf{T}_0, \mathbf{P}_0 - \mathbf{P}_3\rangle}{15} + \frac{\beta(6-h_1)\langle \mathbf{T}_0, \mathbf{T}_1\rangle}{15(h_2-4)},\\
\frac{\partial \widehat{E_1}}{\partial \beta} =& \frac{\langle \mathbf{T}_1, \mathbf{P}_0 - \mathbf{P}_3\rangle(-4h_1^2h_2 - 3h_1h_2^2 + 16h_1^2 + 30h_2^2 + 60h_1h_2 - 192h_1 - 312h_2 + 768)}{105(h_2-4)^2} +\\
& \frac{\alpha(-7h_1h_2 - 14h_1 - 21h_2 - 168)\langle \mathbf{T}_0, \mathbf{T}_1\rangle + \beta(2h_1^2 + 9h_2^2 + 6h_1h_4 - 2h_1 - 5h_2 + 576)}{105(h_2-4)^2},
\end{aligned}$$

α and β can be solved as functions of h_1 and h_2:

$$\begin{aligned}
\alpha_1 = \alpha(h_1, h_2) &= \frac{-\langle \mathbf{P}_0 - \mathbf{P}_3, \mathbf{T}_0\rangle(h_1^2h_2 + 6h_1h_2^2 - 44h_1h_2 + 32h_1 - 60h_2 + 384)}{3h_1^2 + 8h_1h_2 - 68h_1 + 24h_2^2 - 240h_2 + 684},\\
\beta_1 = \beta(h_1, h_2) &= \frac{\langle \mathbf{P}_0 - \mathbf{P}_3, \mathbf{T}_1\rangle(h_2-4)(4h_1h_2 - 40h_2 - 50h_1 + 3h_1^2 + 256)}{3h_1^2 + 8h_1h_2 - 68h_1 + 24h_2^2 - 240h_2 + 684}.
\end{aligned}$$

Using the same method, from

$$\frac{\partial \widehat{E}_2}{\partial \alpha} = \frac{\partial \widehat{E}_2}{\partial \beta} = 0,\ \frac{\partial \widehat{E}_3}{\partial \alpha} = \frac{\partial \widehat{E}_3}{\partial \beta} = 0$$

we can also drive

$$\begin{aligned}
\alpha_2 = \alpha(h_1, h_2) &= \frac{\langle \mathbf{P}_0 - \mathbf{P}_3, \mathbf{T}_0\rangle(2h_1^2h_2 - 2h_1^2 - 2h_1h_2^2 - 14h_1h_2 + 16h_1 + 27h_2^2 - 108h_2 + 216)}{-4h_1^2 + 8h_1h_2 + 16h_1 - 19h_2^2 + 104h_2 - 256},\\
\beta_2 = \beta(h_1, h_2) &= \frac{\langle \mathbf{P}_0 - \mathbf{P}_3, \mathbf{T}_1\rangle(h_2-4)(20h_1 + 3h_2 - 4h_1h_2 - 4h_1^2 - 84)}{-4h_1^2 + 8h_1h_2 + 16h_1 - 19h_2^2 + 104h_2 - 256},\\
\alpha_3 = \alpha(h_1, h_2) &= \frac{-\langle \mathbf{P}_0 - \mathbf{P}_3, \mathbf{T}_0\rangle(2h_1 + 5h_2 - h_1h_2 - 8)}{h_2 - h_1 + 2},\\
\beta_3 = \beta(h_1, h_2) &= \frac{-\langle \mathbf{P}_0 - \mathbf{P}_3, \mathbf{T}_1\rangle(h_1-3)(h_2-4)}{h_2 - h_1 + 2}.
\end{aligned}$$

As a result, we reformulate the minimization problem as

$$\min_{h_1,h_2}\{\overline{E}_i(h_1, h_2) := \widehat{E}_i(h_1, h_2, \alpha_i, \beta_i)\}$$

and Algorithm 1 can be adopted to solve the minimization problem.

Theorem 3.5 *The minimum point of* $\overline{E}_2(h_1, h_2)$ *and* $\overline{E}_3(h_1, h_2)$ *is* $(h_1, h_2) = (3, 1)$.

Proof It can be easily checked that

$$\overline{E}_2(h_1,h_2)-\overline{E}_2(3,1)=\frac{4[\beta_2(h_2-h_1+2)\mathbf{T}_1+(h_1h_2-3h_2-4h_1+12)(\mathbf{P}_0-\mathbf{P}_3)]^2}{5(h_2-4)^2}$$

and

$$\overline{E}_3(h_1,h_2)-\overline{E}_3(3,1)=\frac{48[\beta_3(h_2-h_1+2)\mathbf{T}_1+(h_1h_2-3h_2-4h_1+12)(\mathbf{P}_0-\mathbf{P}_3)]^2}{(h_2-4)^2}.$$

We can know that $\overline{E}_2(h_1,h_2)\geq\overline{E}_2(3,1)$ and $\overline{E}_3(h_1,h_2)\geq\overline{E}_3(3,1)$. Therefore, $(h_1,h_2)=(3,1)$ is the minimum point of $\overline{E}_2=\overline{E}_2(h_1,h_2)$ and $\overline{E}_3=\overline{E}_3(h_1,h_2)$. □

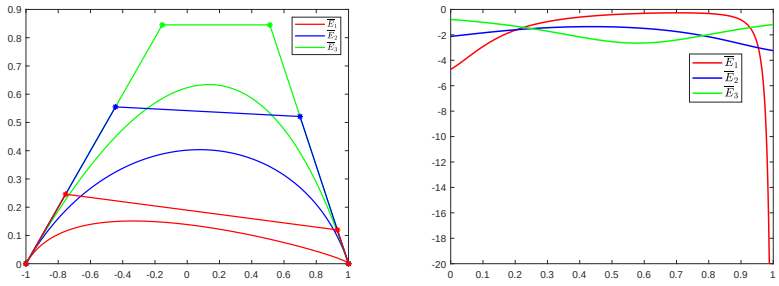

(a) $\mathbf{P}_0=(-1,0)$, $\mathbf{P}_3=(1,0)$, $\mathbf{T}_0=(\cos(\frac{\pi}{4}),\sin(\frac{\pi}{4}))$, $\mathbf{T}_1=-(\cos(-\frac{\pi}{3}),\sin(-\frac{\pi}{3}))$

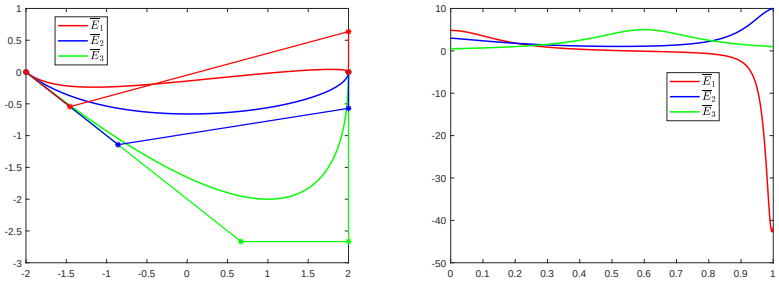

(b) $\mathbf{P}_0=(-2,0)$, $\mathbf{P}_3=(2,0)$, $\mathbf{T}_0=(\cos\frac{3\pi}{4},\sin\frac{3\pi}{4})$, $\mathbf{T}_1=-(\cos\frac{\pi}{2},\sin\frac{\pi}{2})$

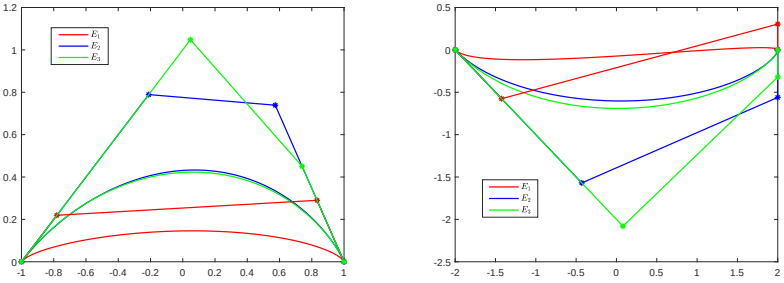

(c) The method in [19] with condition (a) (d) The method in [19] with condition (b)

Figure 5 Example 3.6

Example 3.6 Figure 5 gives two representative examples for the problem of G^1 Hermite Bézier-like curves with energy constraints. By Theorem 3.5, the G^1 Bézier-like curves with minimal

$\overline{E}_2$ or $\overline{E}_3$ energy is just the G^1 Bézier curve with $h_1 = 3, h_2 = 1$. Given the control points $\mathbf{P}_0$, $\mathbf{P}_1$ and tangent vectors $\mathbf{T}_0$, $\mathbf{T}_1$, the parameters h_1, h_2 of the G^1 Bézier-like curves with minimal $\overline{E}_1$ energy can be obtained by Algorithm 1. Comparison with the method in [19] on Bézier-like curves with $h_1 = 2$ and $h_2 = 3$ by minimizing energy E_1, E_2, E_3 is also presented in Figure 5. It is obvious that our method of G^1 Bézier-like curves with minimal internal energy and proper parameters has lower internal energy. The comparative energies and curvature information can be found in Table 3.

Energy	h_1	h_2	$\overline{E}_1$	$\overline{E}_2$	$\overline{E}_3$	AC	Energy	$h_1 = 2$, $h_2 = 3$
$\overline{E}_1$(3.4(a))	3.6588	3	4.6051	32.7291	449.3505	-1.9105	E_1(3.4(c))	4.7539
$\overline{E}_2$(3.4(a))	3	1	5.0200	17.1898	74.2483	-1.8343	E_2(3.4(c))	25.0968
$\overline{E}_3$(3.4(a))	3	1	6.2393	26.8719	0	-1.8309	E_3(3.4(c))	353.8470
$\overline{E}_1$(3.4(b))	3.8300	3	18.3439	142.8508	2081.1596	-0.8204	E_1(3.4(d))	19.1975
$\overline{E}_2$(3.4(b))	3	1	20.3755	109.7142	858.1224	2.3645	E_2(3.4(d))	129.4355
$\overline{E}_3$(3.4(b))	3	1	42.6667	320.0000	0	2.3530	E_3(3.4(d))	1873.9200

Table 3 Comparison of different curves in Figure 5

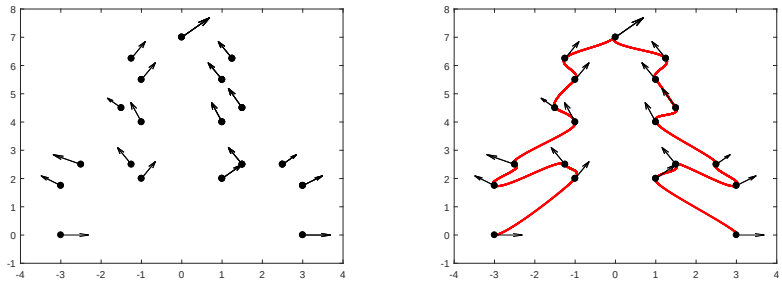

(a) Input data (b) G^1 interpolating curve

Figure 6 Shape design

Furthermore, Figure 6 presents an application of our method to shape design, since it can conveniently display the intended interpolation effects. In Figure 6, the G^1 interpolating spline curve with minimal $\overline{E}_1$ is constructed to match the specified input data (an ordered set of points with tangent vectors).

4. Conclusion

To make the curves have better shape adjustability and approximation, a novel class of Bernstein-like basis functions and Bézier-like curves are proposed. Since the construction of curves satisfying certain constraints has important theoretical significance, we construct the Bézier-like curves with energy constraints. Moreover, the construction of planar C^1 and G^1 Hermite Bézier-like curves via energy minimization are studied. Our method is mainly used to achieve the ideal result of curve design by searching the optimal value of two parameters h_1, h_2

in the feasible region. Examples and applications of the method to shape design are also outlined to illustrate efficiency.

Acknowledegments We thank the editor and the referees for their time and valuable comments.

References

[1] G. FARIN. *Curves and Surfaces for CAGD: A Practical Guide*. Academic Press, Fifth Edition, San Diego, 2002.

[2] Xi-an HAN, Xili HUANG, Yichen MA. *Shape analysis of cubic trigonometric Bézier curves with a shape parameter*. Appl. Math. Comput., 2010, **217**(6): 2527–2533.

[3] Lanlan YAN, Jiongfeng LIANG. *An extension of the Bézier model*. Appl. Math. Comput., 2011, **218**(6): 2863–2879.

[4] Qinyu CHEN, Guozhao WANG. *A class of Bézier-like curves*. Comput. Aided Geom. Design, 2003, **20**(1): 29-39.

[5] Gang HU, Huanxin CAO, Suxia ZHANG, et al. *Developable Bézier-like surfaces with multiple shape parameters and its continuity conditions*. Appl. Math. Model., 2017, **25**: 728–747.

[6] Gang XU, Guozhao WANG, Wenyu CHEN. *Geometric construction of energy-minimizing Bézier curves*. Sci. China Inf. Sci., 2011, **54**(7): 1395–1406.

[7] J. MONTERDE. *Bézier surfaces of minimal area: the Dirichlet approach*. Comput. Aided Geom. Design, 2004, **21**(2): 117–136.

[8] Y. J. AHN, C. HOFFMANN, P. ROSEN. *Geometric constraints on quadratic Bézier curves using minimal length and energy*. J. Comput. Appl. Math., 2014, **255**: 887–897.

[9] Lizheng LU. *Planar quintic G^2 Hermite interpolation with minimum strain energy*. J. Comput. Appl. Math., 2015, **274**: 109–117.

[10] Lizheng LU, Chengkai JIANG, Qianqian HU. *Planar cubic G^1 and quintic G^2 Hermite interpolations via curvature variation minimization*. Comput. Graph., 2018, **70**: 92–98.

[11] R. J. CRIPPS, M. Z. HUSSAIN. *C^1 monotone cubic Hermite interpolant*. Appl. Math. Lett., 2012, **25**(8): 1161–1165.

[12] T. HAGSTROM, D. APPELÖ. *Solving PDEs with Hermite Interpolation*. Springer, Cham, 2015.

[13] Juncheng LI. *Constructing planar C^1 cubic Hermite interpolation curves via approximate energy minimization*. J. Math. Res. Appl., 2019, **39**(4): 433–440.

[14] R. VELTKAMP, W. WESSELINK. *Modeling 3D curves of minimal energy*. Comput. Graph. Forum., 1995, **14**(3): 97–110.

[15] V. A. TOPONOGOV. *Differential Geometry of Curves and Surfaces: A Concise Guide*. Basel, Birkhäuser, 2006.

[16] D. BERTSEKAS. *Nonlinear Programming*. 2nd ed. Belmont, Athena Scientific, 1999.

[17] P. TSENG. *Convergence of a block coordinate descent method for nondifferentiable minimization*. J. Optim. Theory Appl., 2001, **109**(3): 475–494.

[18] R. T. FAROUKI, T. SAKKALIS. *Pythagorean hodographs*. IBM J. Res. Develop., 1990, **34**(5): 736–752.

[19] Zhihong HAN, Chungang ZHU. *Construction of Bézier curves by energy constraints*. J. Computer-Aided Design & Computer Graphics, 2020, **32**(2): 213–221.